

Spin-glass behavior in an antiferromagnetic frustrated spinel: $\text{ZnCr}_{1.6}\text{Ga}_{0.4}\text{O}_4$

D. Fiorani and S. Viticoli

Istituto di Teoria, Struttura Elettronica e Comportamento Spettrochimico dei Composti di Coordinazione del Consiglio Nazionale delle Ricerche—Area della Ricerca di Roma, Via Salaria Km 29.5 Casella Postale 10, I-00016 Monterotondo Stazione (Roma), Italy

J. L. Dormann

Laboratoire de Magnétisme, Centre National de la Recherche Scientifique, 1 place A. Briand, F-92190 Meudon (Bellevue), France

J. L. Tholence

Centre de Recherches sur les très basses Températures, Centre National de la Recherche Scientifique, Boîte Postale 166X, F-38042 Grenoble Cedex, France

A. P. Murani

Institute Laue Langevin, F-38042 Grenoble Cedex, France

(Received 2 March 1983; revised manuscript received 30 January 1984)

A study of magnetic properties in the insulating spinel $\text{ZnCr}_{1.6}\text{Ga}_{0.4}\text{O}_4$ (chromium ions in octahedral sites) has been made by carrying out low-field dc- and ac-susceptibility measurements as well as neutron diffraction, Mössbauer, and EPR experiments, which all give evidence of spin-glass-like behavior. The topological frustration, connected with the high ground-state degeneracy of the antiferromagnetic spinel octahedral sublattice, is the origin of the spin-glass ordering. Strong nearest-neighbor antiferromagnetic interactions are dominant in the system, leading to short-range magnetic order which appears at temperatures much higher than the freezing temperature defined by the ac-susceptibility cusp [$T(\nu=17\text{ Hz})=2.50\text{ K}$ is frequency dependent]. The thermoremanent magnetization does not vanish at T_f , suggesting the existence of uncompensated clusters blocked above T_f . A paramagnetic behavior is observed below $T=1\text{ K}$, providing evidence for the presence of unfrozen spins below T_f (entropic clusters).

I. INTRODUCTION

Bond frustration has been identified as being the origin of spin-glass behavior.¹ In a metallic spin-glass the frustration character is related to the oscillatory form of the Ruderman-Kittel-Kasuya-Yosida (RKKY) interaction. In these and in the insulating spin-glasses, where the magnetic interactions are predominantly short range and not mediated by the conduction electrons, the frustration may be due to the competition between interactions of different signs [i.e., $\text{Eu}_x\text{Sr}_{1-x}\text{S}$ (Ref. 2)] or it may be inherent in the underlying lattice in a system with only antiferromagnetic interactions [e.g., fcc lattices $\text{Cd}_{1-x}\text{Mn}_x\text{Te}$ (Refs. 3–5) and $\text{Hg}_{1-x}\text{Mn}_x\text{Te}$ (Ref. 6)].^{7,8}

Randomly substituted solid solutions with spinel structure, which have magnetic moments only on octahedral sites, offer further examples of both types of frustration (competing interactions and topological frustration) that are possible in insulating spin-glasses. Indeed, spin-glass behavior has been recently found in the thiospinels $\text{CdIn}_{2-2x}\text{Cr}_{2x}\text{S}_4$ (Ref. 9–13) and $\text{ZnAl}_{2-2x}\text{Cr}_{2x}\text{S}_4$ (Refs. 9 and 10), due to the simultaneous presence of competing ferromagnetic [nearest-neighbor (NN)] and antiferromagnetic [next-nearest-neighbor (NNN)] interactions.

In this paper, we present experimental evidence of spin-glass behavior in the oxispinel $\text{ZnCr}_{1.6}\text{Ga}_{0.4}\text{O}_4$, in

which all of the interactions are antiferromagnetic and predominantly short range, and the frustration is inherent in the lattice.¹⁴

The B sites of the spinel lattice form tetrahedra and each site is common to two tetrahedra (Fig. 1). The character of the frustration of the octahedral antiferromagnetic sublattice (magnetic ions, antiferromagnetically coupled, on B sites only) with only NN interactions was stressed by Anderson¹⁵ and more recently by Villain.⁸ Many configurations having the same energy are possible, the ground state being determined by the condition that all tetrahedra separately have their energy minimized (associating the four spins in two antiparallel pairs). The

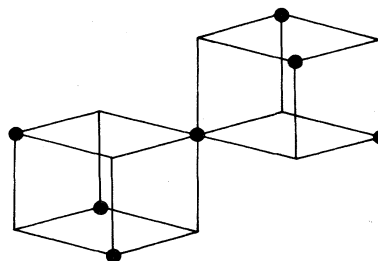


FIG. 1. Octahedral sites of the spinel lattice with first-nearest neighbors.

high ground-state degeneracy would prevent any long-range order from being established. The term "cooperative paramagnet" has been used to describe the resulting magnetic state.⁸

In the real systems the ground-state degeneracy can be reduced in several ways, e.g., from lattice distortions, as in MgCr_2O_4 and ZnCr_2O_4 , which order antiferromagnetically with tetragonal distortion below T_N .¹⁶⁻²⁰ Moreover, although weaker by an order of magnitude, the superexchange interactions with more distant neighbors are nevertheless non-negligible, and are believed to be responsible for the variety of magnetic structures observed at low temperatures in this kind of spinel.²¹

The ground-state degeneracy can also be reduced by defects, e.g., nonmagnetic impurities, whose presence in sufficient number can stabilize a spin-glass phase, as suggested by Villain.⁸

The magnetic phase diagram proposed by Villain,⁸ assuming the presence of only NN interactions, has been recently discussed, and a modified form has been suggested, taking into account the experimental results for real systems, which includes the presence of an antiferromagnetic phase for the pure magnetic B spinel, as well as for high concentrations of magnetic B ions.²²

ZnCr_2O_4 is an antiferromagnet ($T_N=13$ K) with very strong antiferromagnetic interactions ($\Theta=-392$ K),²³ predominantly between nearest neighbors.

We have experimentally verified that the introduction of 20% of substitutional nonmagnetic impurities (Ga^{3+} ions) in the octahedral sites of ZnCr_2O_4 produces a spin-glass phase. The observation of a spin-glass state for $x=0.80$, while the percolation threshold for antiferromagnetism in the octahedral spinel sublattice is 0.40,^{24,25} reflects the high degree of frustration present in the lattice.

The magnetic study of the spinel $\text{ZnCr}_{1.6}\text{Ga}_{0.4}\text{O}_4$ has been carried out by low-field dc- and ac-susceptibility measurements, neutron-diffraction experiments, and Mössbauer and EPR spectroscopy.

II. EXPERIMENTAL SETUP

ZnCr_2O_4 and ZnGa_2O_4 , both normal spinels, form solid solutions throughout the entire concentration range, as shown by x-ray diffraction, with gallium atoms replacing chromium atoms in octahedral sites.²⁶⁻²⁸

A. Preparation

Polycrystalline $\text{ZnCr}_{1.6}\text{Ga}_{0.4}\text{O}_4$ was prepared starting from a mixture of the oxides ZnO (99.99% pure), Cr_2O_3 (99.999% pure), and Ga_2O_3 (99.9997% pure) (Koch-Light) following the procedure reported elsewhere (annealing at $T=800$ C for 1 d, then grinding and reannealing at 1200°C for 2 d).²⁶ This annealing was followed by a slow cooling (12 h) to room temperature. An iron-doped sample (1 at.% ^{57}Fe of the total chromium content) for Mössbauer spectra was prepared in the same way, adding $^{57}\text{Fe}_2\text{O}_3$ to the starting oxide mixture. X-ray diffraction shows that both samples powder are composed of a single-phase spinel with a lattice parameter a

$= (8.330 \pm 0.001) \text{ \AA}$. The fact that we have a powder sample can influence the low-temperature irreversible properties.

B. Susceptibility measurements

Low-field dc-susceptibility measurements were performed in the temperature range $0.05 \leq T \leq 4.20$ K by an extraction method using an apparatus provided with an adiabatic demagnetization described elsewhere.²⁹ High-field ($H=8.4$ kOe) susceptibility measurements were performed in the temperature range $4.2 \leq T \leq 100$ K using a Faraday balance described elsewhere.³⁰ ac-susceptibility measurements were performed in the temperature range $1.5 \leq T \leq 4.2$ K, using a mutual inductance bridge at $\nu=17$ and 198 Hz.

C. Neutron-diffraction measurements

Neutron-scattering experiments were performed on the D2 diffractometer at The Institut Laue-Langevin (Grenoble) using neutrons of wavelength 2.37 Å with the Ge(111) monochromator. At this wavelength there is a small contamination giving additional Bragg peaks of weak intensity. The measurements were carried out as a function of temperature from room temperature to $T=1.5$ K, the lowest temperature attainable with the ^4He cryostat used.

D. Mössbauer spectra

Mössbauer experiments were carried out as a function of temperature ($T \geq 1.8$ K) on the ^{57}Fe -doped sample using a conventional spectrometer operated in the constant-acceleration mode. The source was ^{57}Co in Pt.

E. EPR spectra

The EPR spectra were recorded at X-band frequency in the temperature range $4.2 \leq T \leq 300$ K using a Varian E9 spectrometer with an Oxford continuous-flow cryostat (ESR19).

III. RESULT AND DISCUSSION

Low-field dc- and ac-susceptibility measurements, neutron-diffraction experiments, and Mössbauer-effect measurements have allowed the magnetic phase diagram of the $\text{ZnCr}_{2x}\text{Ga}_{2-2x}\text{O}_4$ spinel system²⁷ to be derived (Fig. 2). Here we report a detailed magnetic study for the composition $x=0.80$, which is in the spin-glass region.

A. Low-field dc-susceptibility measurements

Low-field dc-susceptibility measurements were performed in the temperature range $0.5 \leq T \leq 4.20$ K as follows: the sample was field-cooled ($H=300$ Oe) and at each temperature two magnetizations were measured: $M(H,T)$, the magnetization at the field H , and the remanent magnetization $M_r(H,T,t)$ measured at zero field after suppression of the cooling field.

Two susceptibilities were deduced corresponding to the

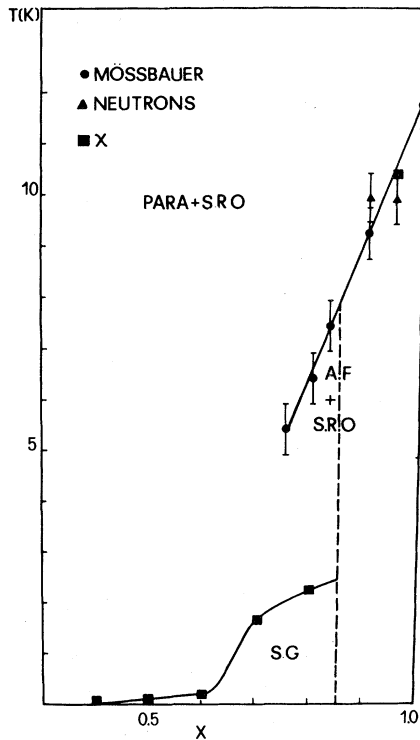


FIG. 2. Simplified version of magnetic phase diagram of $\text{ZnCr}_{2x}\text{Ga}_{2-2x}\text{O}_4$.

linear regime of M versus H : the total field-cooled susceptibility $\chi_T = M/H$, and the reversible susceptibility, $\chi_{\text{rev}} = (M - M_r)/H$.

The susceptibility curve (Fig. 3) shows a spin-glass behavior, the reversible susceptibility $\chi_{\text{rev}}(t_m = 40 \text{ s})$ exhib-

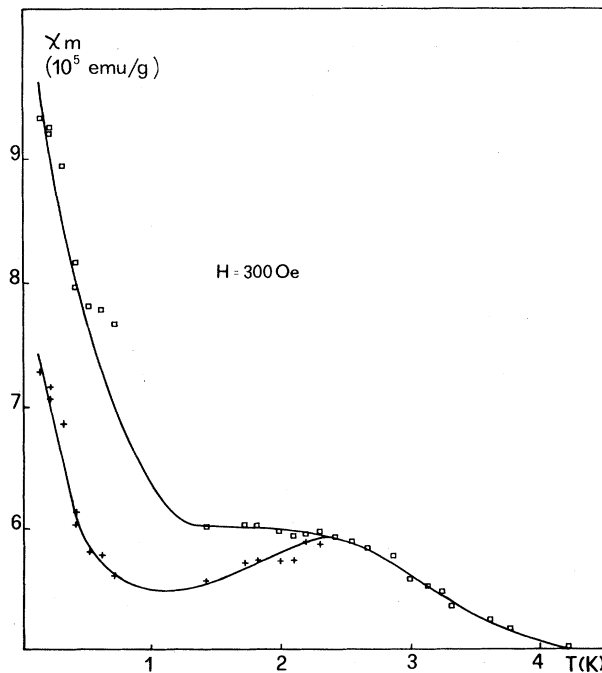


FIG. 3. Temperature dependence of the low-field dc susceptibility. +, $\chi_{\text{rev}} = [(M(H = 300 \text{ Oe}) - M_r)/H(300 \text{ Oe})]$; \square , $\chi_T = M(H = 300 \text{ Oe})/H(300 \text{ Oe})$.

its a peak at $T_f = (2.40 \pm 0.05) \text{ K}$, while the total (field-cooled) susceptibility χ_T shows no discontinuity, being almost independent of the temperature below T_f , except for a slight increase with decreasing temperature.

At lower temperature (below 1 K) the susceptibilities again increase. Below the freezing temperatures the susceptibility is described by the law

$$\chi = \chi_0 + \alpha T + \frac{c}{T - \Theta},$$

which is the sum of following contributions. (a) $\chi_0 + \alpha T$: this term is assumed to represent the spin-glass contribution, constituted by a constant term χ_0 ($= 7.7 \times 10^{-3} \text{ emu/mol Cr}^{3+}$), which should represent the $T \rightarrow 0$ limit of χ in the absence of low-temperature paramagnetic behavior, and a term varying with temperature αT ($\alpha = 5.1 \times 10^{-3}$), which would represent the usual spin-glass contribution to the susceptibility below T_f , assuming that it is proportional to T . (b) a paramagnetic term $C/(T - \Theta)$ ($C = 5.9 \times 10^{-3}$; $\Theta = -0.04 \text{ K}$).

The paramagnetic contribution reveals the existence of a residual fraction of unfrozen spins below T_f . These spins may not be truly isolated spins (considering the very high chromium concentration), but instead interacting spins for which the internal fields, coming from their neighbors, cancel or at least give a resultant lower than the thermal energy KT ($H < (KT/\mu) \simeq 200 \text{ Oe}$, $T = 50 \text{ mK}$ being the lowest measuring temperature). At lower temperatures a blocking of these spins is possible, as observed in $\text{Eu}_x\text{Sr}_{1-x}\text{S}$.³¹⁻³⁴

For paramagnetic chromium spins ($S = \frac{3}{2}$), the Curie constant is given by

$$C_0 = \frac{N_0 S(S+1)g^2 \mu_B^2}{3k_B} = 1.875.$$

There, (the experimental value of C ($= 7.3 \times 10^{-3}$) would correspond to a fraction $N/N_0 = 4 \times 10^{-3}$ of loose chromium spins, if they were considered truly independent entities with $S = \frac{3}{2}$. These loose entities may be spins grouped in clusters, which should have an almost-compensated average magnetic moment. In that case, N'/N is then an underestimated concentration of single spins. One notes that the fraction of truly isolated spins predicted for a statistical distribution at this concentration is negligible (5×10^{-5}), representing only 1% of the loose chromium spins calculated as above.

The existence of these observed loose spins has been theoretically predicted in frustrated systems. Investigations by computer simulation of the ground states³⁵ and low-energy excited states³⁶ of several periodical models have shown the presence of a number of spins which experience an effective field equal to 0 (entropic clusters). These entropic clusters are readily reversed, flipping spin by spin at constant energy, with the mean reversal time τ_r depending only on the square of the number of spins.³⁶ They are predicted to provide a Curie-type contribution to the observed susceptibility, as found in our system and $\text{Cd}_{1-x}\text{Mn}_x\text{Te}$ (Refs. 4 and 5) below T_f .

Static susceptibility measurements were also performed below $T = 4.2 \text{ K}$ using higher cooling fields (see Fig. 4 for $H = 2.9 \text{ kOe}$). The effect of using a high cooling field is

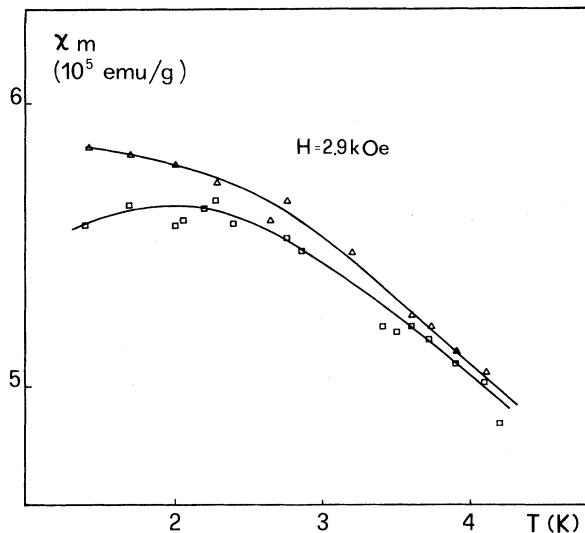


FIG. 4. Temperature dependence of dc susceptibility. \square , $\chi_{\text{rev}} = [M(H=2.9 \text{ kOe}) - M_r]/H(2.9 \text{ kOe})$; \triangle , $\chi_T = M(H=2.9 \text{ kOe})/H(2.9 \text{ kOe})$.

to round off the maximum of χ_{rev} and to shift it to lower temperatures. Moreover, the behavior of χ_T is also strongly modified, continuously increasing with decreasing temperature. It is known that an increase of the cooling field produces a decrease of M/H and a gradual disappearance of the discontinuity at T_f , when present. A discontinuity of χ_T around T_f has been observed in concentrated $\text{Cu}_{1-x}\text{Mn}_x$ ($x=1.2$ at. %) (Ref. 37), while a slow increase of χ_T has been observed below T_f in $\text{La}_{1-x}\text{Gd}_x\text{Al}_2$ (Ref. 38) (where the amplitude V of the RKKY interaction is much smaller) and in very dilute $\text{Cu}_{1-x}\text{Mn}_x$ (Ref. 39). These differences may be attributed to the strong sensitivity of the anomaly to the applied dc field (H/x), which is characteristic of the system (experi-

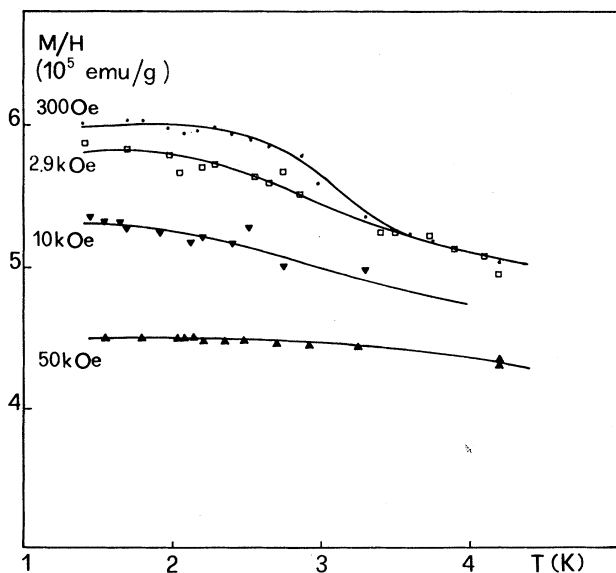


FIG. 5. Temperature dependence of dc susceptibility for different cooling fields: \bullet , $H=300$ Oe; \square , $H=2.9$ kOe; \blacktriangledown , $H=10$ kOe; \blacktriangle , $H=50$ kOe.

mentally, it is found that the upper field limit for observing such discontinuity varies with the system and concentration).

In Fig. 5 the behavior of χ_T with the temperature is reported for various field values including $H=10$ and 50 kOe. Upon cooling under $H=50$ kOe, χ_T becomes almost constant below 4.2 K.

B. High-field dc-susceptibility measurements

High-field ($H=8.4$ kOe) dc-susceptibility measurements were performed in the temperature range $4.2 \leq T \leq 100$ K after zero-field cooling. $M(H)$ is always linear in these field and temperature ranges.

Strong deviations from Curie-Weiss behavior, which increase with decreasing temperature, are clearly observed from temperatures far above T_f (Fig. 6). Measurements up to higher temperatures than presently studied would be necessary to attain a pure Curie-Weiss behavior and hence to correctly deduce the Curie constant C and the asymptotic Curie-temperature (Θ) value. Nevertheless, the high negative intercept on the temperature axis of the straight line observed at higher temperatures clearly shows that strong antiferromagnetic interactions are present [for the pure compound ZnCr_2O_4 , $\Theta = -392$ K (Ref. 23)].

The observed behavior of the susceptibility demonstrates that strong short-range correlations among chromium spins are established far above T_f , as confirmed by neutron-diffraction experiments and EPR spectra (see below), and evolve with decreasing temperature, leading to the gradual growth of uncompensated clusters, bearing a weak moment, which have properties similar to antiferromagnetic superparamagnetic particles. Indeed, the progressive increase with decreasing temperature of the slope $d\chi^{-1}/dT$, equal to $1/C$ in the paramagnetic re-

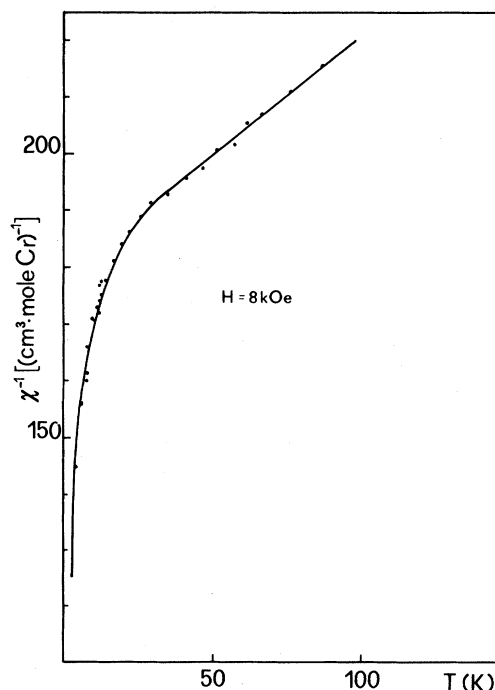


FIG. 6. Temperature dependence of dc susceptibility ($H=8.4$ kOe).

gime, reflects a progressive decrease of the apparent Curie constant, which is as expected if the magnetic moments of these clusters with antiferromagnetic interactions are smaller than $n^{1/2}\mu$ (n is the number of spins in the cluster).

C. Frequency dependence of T_f

ac-susceptibility measurements performed in the temperature range $1.5 \leq T \leq 4.2$ K at $\nu=17$ and 198 Hz showed a peak at $T=(2.50 \pm 0.05)$ and (2.65 ± 0.05) K, respectively (Fig. 7). The freezing temperature derived from χ_{dc} measurements by the extraction method ($t_m=40$ s) is $T_f=2.40$ K.

The frequency sensitivity of the spin-glass transition, defined as the relative variation $\Delta T_f/T_f$ per decade of time in a given frequency range is $\Delta T_f/(T_f \Delta \ln \nu) = 5 \times 10^{-2}$. The frequency dependence of T_f has been found to follow scaling laws in a metallic spin-glass,^{40,41} while a concentration dependence of $\Delta T_f/(T_f \Delta \ln \nu)$ has been reported for insulating ones (i.e., $\text{Eu}_x\text{Sr}_{1-x}\text{S}$).⁴⁰ In any case, the frequency sensitivity found for our sample is 1 order of magnitude higher than those reported for canonical spin-glasses, i.e., CuMn (Refs. 40–42) and AgMn (Refs. 40–43), for which a concentration-independent value of 5×10^{-3} is reported. This fact suggests a less cooperative freezing in our insulating spin-glass, where the interactions are predominantly short ranged.

D. Remanent magnetization

The behavior of the thermoremanence with the temperature T , the time t , and the cooling field H has been studied.

The thermal variation of the thermoremanent magnetization is reported in Fig. 8 for different cooling fields H .

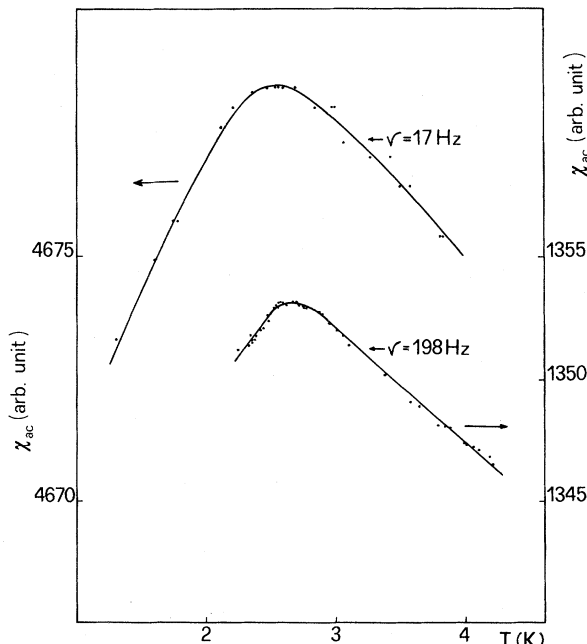


FIG. 7. Temperature dependence of the ac susceptibility for $\nu=17$ and 198 Hz.

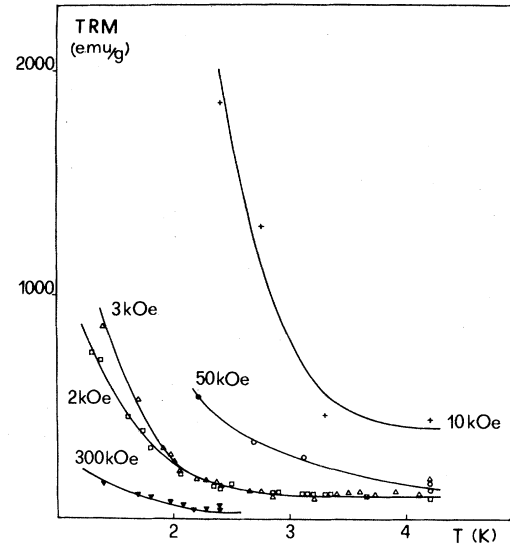


FIG. 8. Thermoremanent magnetization M_{TR} as a function of the temperature for different cooling fields. ∇ , $H=300$ Oe; \square , $H=2.0$ kOe; \triangle , $H=3.0$ kOe; $+$, $H=10$ kOe; \circ , $H=50$ kOe.

An exponential law of the type $M_{TR}(T, H, t) = M_{TR}(0) \exp(-\beta T)$ is followed (Fig. 9) with a coefficient increasing with the cooling field [$\beta(H=0.3$ kOe)=1.49; $\beta(H=2.0$ kOe)=1.64; $\beta(H=3.0$ kOe)=2.19]. M_{TR} persists above T_f , continuing to follow an exponential behavior with a lower coefficient. The change of slope in the plot $\ln M_{TR}$ versus T corresponds to the freezing-temperature value determined by χ_{dc} measurements ($T_f=2.40$ K). The high-temperature part of M_{TR} corre-

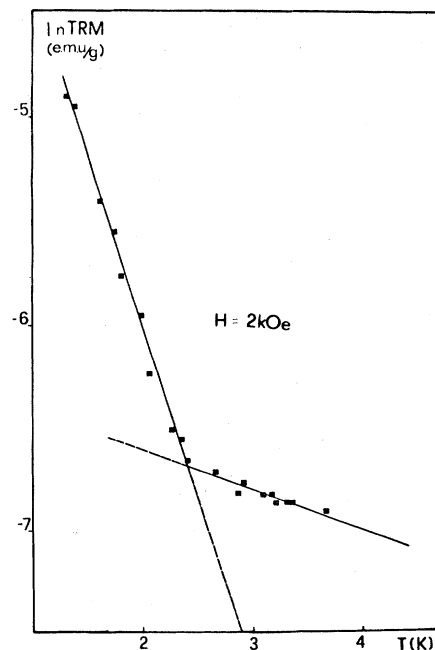


FIG. 9. Temperature dependence of the thermoremanent magnetization $M_{TR} \sim \exp(-\beta T)$ in a semilogarithmic plot for $H=2.0$ kOe.

sponds to the blocking of some remaining antiferromagnetic clusters (whose existence is later shown through Mössbauer experiments). Then, when one enters the spin-glass regime ($T < 2.4$ K), the more rapid increase of M_{TR} is associated with the coupling between clusters. The same type of behavior has been found in the case of very small interacting particles.⁴⁴⁻⁴⁶

The time dependence of M_{TR} follows a power law of the type $M_{\text{TR}}(T, H, t) = M_{\text{TR}}(T, H, 0)t^{-\alpha}$. The exponent α is field dependent: $\alpha(H = 2.0 \text{ kOe}) = 5.3 \times 10^{-2}$; $\alpha(H = 2.9 \text{ kOe}) = 6.8 \times 10^{-2}$, increasing with the field (Fig. 10). A power law to describe the relaxation of M_{TR} was initially proposed in the literature on the basis of Monte Carlo simulations⁴⁷ and was experimentally verified (in a given range of time and temperature) on some system, i.e., $\text{Eu}_{0.4}\text{Sr}_{0.6}\text{S}$.^{48,49} In that system the coefficient was found to increase with field, tending to a saturation value and divergence for temperatures approaching T_f .

The observed thermal variation and time dependence of M_{TR} seems consistent with a thermally activated blocking process described by an Arrhenius law. Indeed, the time and the temperature dependence of M_{TR} can be described by the relation $M_{\text{TR}}(T, t, H) = M_{\text{TR}}(0)\exp(-AT \ln BT)$ (A and B are constant) which associates the time and the temperature dependence in a single variable. The measurements were performed below T_f down to $T = 1.3$ K and the time evolution was followed up to $t = 50$ min.

The general behavior observed for the saturated thermoremanent magnetization in spin-glasses is $M_{\text{TR}}^S(T, t) = M_{\text{TR}}^S(0)\exp[-(T/T_0)\ln(t/\tau_0)]$. This relation was found to hold in the temperature range between $\frac{1}{3}T_f$ and $\frac{2}{3}T_f$.^{50,51} In our case the applied field was lower than the saturating value.

The field dependence of M_{TR} and M_{IR} (isothermal remanent magnetization) is reported in Fig. 11. The saturating-field value should be higher than 40 kOe. The unusual maximum of M_{TR} could be explained by considering the quite large application time of the field (2 min), as suggested in other cases.⁵² Indeed, it is known that for an increasing application time of the field H , M_{TR} tends to M_{TR} , whose behavior is characterized by the presence of a maximum.

Recently, the field dependence of M_{TR} in spin-glasses

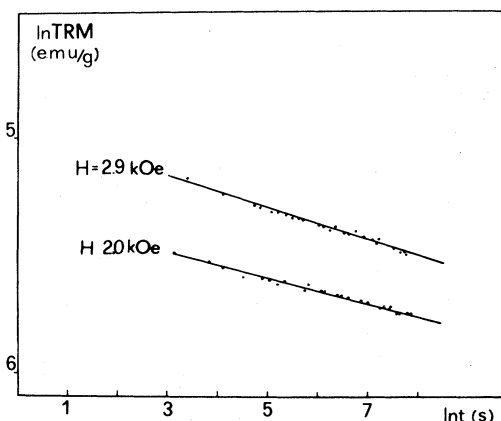


FIG. 10. Time dependence of the thermoremanent magnetization at $T = 1.70$ K; $M_{\text{TR}} \sim t^{-\alpha}$ for two fields.

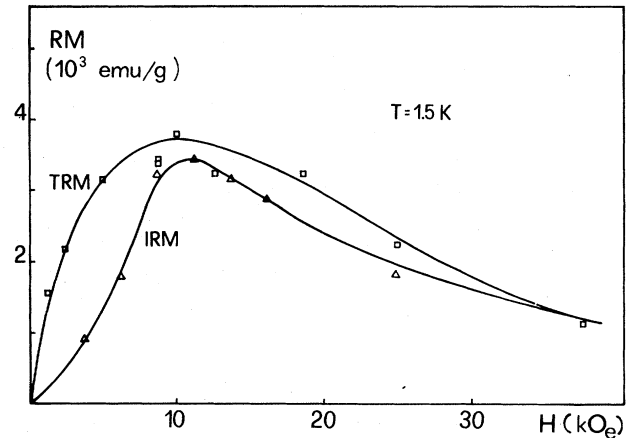


FIG. 11. Isothermal remanent magnetization (M_{IR}) and thermoremanent magnetization (M_{TR}) as functions of the previously applied field at $T = 1.50$ K. The magnetization was measured 1 min after suppressing the field. For M_{IR} measurements the field was applied for 2 min after zero-field cooling.

has been attributed to an homogeneous dynamical effect^{48,49} resulting from the increase of the rate of relaxation with cooling field, in contrast with the inhomogeneous description in terms of clusters with a different activation,⁵³ whose existence is evidenced by Mössbauer spectra in our case (see below).

E. Field-dependent magnetization measurements

The field dependence of the magnetization at $T = 4.2$ K ($T > T_f$) after zero-field cooling is illustrated in Fig. 12. At higher field a deviation from the linearity is observed,

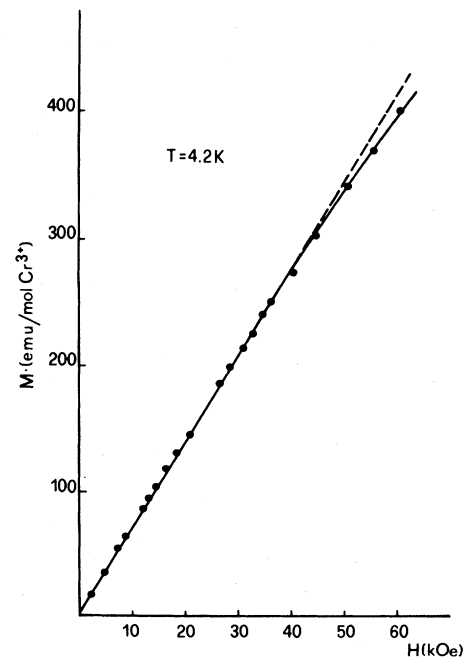


FIG. 12. Field dependence of the magnetization at $T = 4.2$ K after zero-field cooling.

increasing with increasing field. Two types of contributions to the magnetization are present: a contribution coming from extended antiferromagnetic regions and a contribution coming from the orientation of uncompensated magnetic moments (uncompensated clusters of different dimensions), which increases with decreasing chromium concentration. At low fields both are expected to give a magnetization proportional to the field, but at higher fields the susceptibility of the first term does not change, whereas that of the second one decreases with increasing field, because of the orientation of the resulting moment of the clusters in the field direction. This is consistent with the behavior of M/H (Fig. 5) measured as function of the temperature at different fields below $T=4.2$ K, which decreases with increasing field and which becomes almost temperature independent at the highest field ($H=50$ kOe).

F. Neutron-diffraction measurements

The neutron-diffraction pattern at $T=293$ K shows the nuclear Bragg peaks corresponding to the spinel structure, including additional peaks due to the $\lambda/3$ contamination [Fig. 13(a)]. The presence of the strong nuclear Bragg

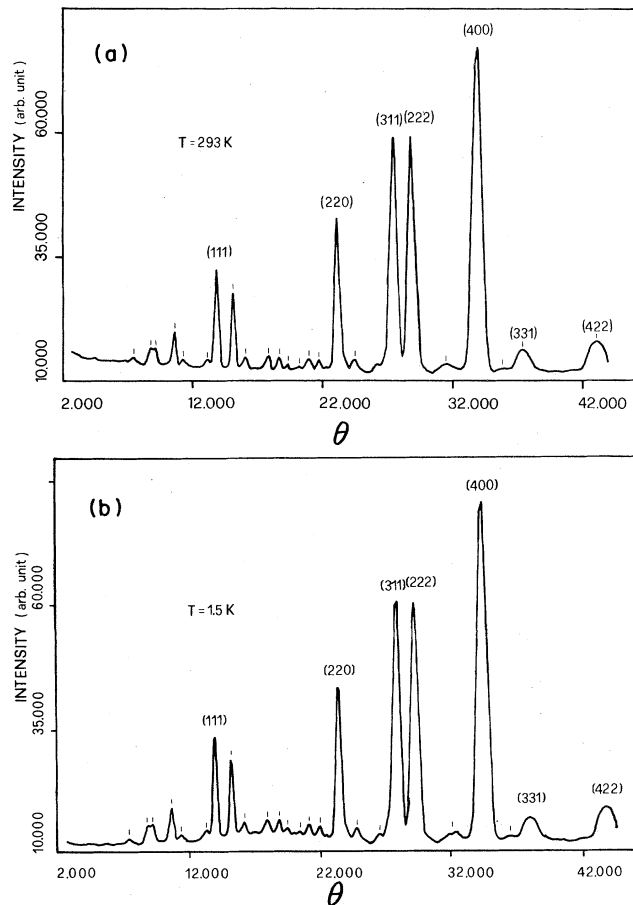


FIG. 13. (a) Neutron-diffraction pattern measured at $T=293$ K as a function of the scattering angle θ . The neutron wavelength was 2.37 Å. The small hashmarks indicate the nuclear peaks arising from the $\frac{1}{3}$ component. (b) Spectrum at $T=1.5$ K measured under the same conditions.

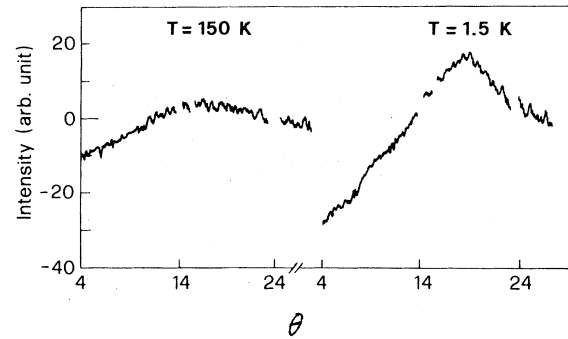


FIG. 14. Difference spectrum ($T-293$) K. The q region of the strong nuclear peaks is omitted in the plots because of the small changes in the lattice constant with temperature, which do not allow an exact subtraction of the spectra.

peaks makes it difficult to ascertain whether some small amount of short-range order is present at this temperature. However, taking the data at $T=293$ K as reference we have determined the evolution of the short-range order by simple subtraction of the 293-K spectrum as background. The results are shown in Fig. 14, where at the lowest temperature ($T=1.5$ K) we observe a strongly developed short-range-order hump peaking between the (111) and (220) reflections. The broad diffuse peak becomes broader and weaker as the temperature is raised, corresponding to the thermal disruption of the magnetic correlations.

For now we have made no attempt to fit the data to the shell models but have, for simplicity, evaluated the height (h) of the broad short-range-order peak as a rough measure of the short-range "order parameter." This, together with the half-width at half-height ($\Delta_{1/2}$) proportional to the inverse correlation length, is shown in Fig. 15. We remark that the evolution of the short-range order is continuous across the spin-glass freezing temperature T_f ($=2.50$ K for $\nu=17$ Hz). Although the height of the short-range-order peak continues to increase down to $T=1.5$ K, the lowest temperature in this study, it is ex-

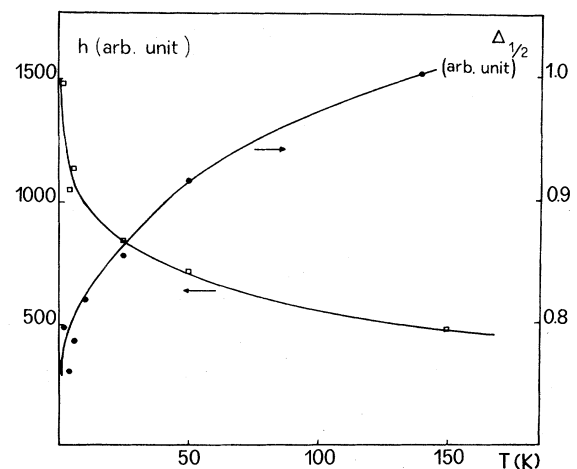


FIG. 15. Temperature dependence of the height (h) and of the half-width at half-height ($\Delta_{1/2}$) of the broad short-range-order peak in the neutron-diffraction spectra.

pected to saturate out at sufficiently low temperatures well below the freezing temperature. We also note that the short-range order is fairly well developed at relatively high temperatures, $T=150$ K, and may even be present at room temperature. This is not surprising since the susceptibility measurements indicate fairly high Curie-Weiss temperatures [$\Theta = -392$ K in ZnCr_2O_4 (Ref. 23)]. Such strong short-range magnetic correlations have been directly observed by polarized scattering techniques at elevated temperatures, much higher than the magnetic ordering temperatures, in systems such as MnSi .⁵⁴

G. Mössbauer spectra

The spectra show a paramagnetic doublet [isomer shift referred to metallic iron at 300 K: $\delta = 0.44$ mm s^{-1} ; quadrupole splitting $eQV_{ZZ}/4 = 0.19$ mm s^{-1} at 77 K (Ref. 27)] down to (6.5 ± 0.5) K, the temperature at which a hyperfine spectrum appears. Below $T=6.5$ K the spectra consist of a superposition of a paramagnetic doublet and an enlarged sextuplet (Fig. 16) whose intensity increases with decreasing temperature down to $T=1.8$ K (Fig. 17) (at this temperature the intensity of the paramagnetic component is less than 2%, the limit of the instrumental precision).

It is not possible to fit the enlarged sextuplet with a simple model. At $T=1.8$ K the model which seems the most appropriate is a distribution of hyperfine fields H_{hyp} , symmetrical with $\langle H_{\text{hyp}} \rangle = 395$ kOe and a width of 90 kOe (at half-height). When the temperature increases, the sextuplet's shape deviates towards that of one largely influenced by relaxation phenomena. Therefore it should be necessary to take into account both phenomena, i.e., relaxation and H_{hyp} distribution, but this procedure is complex and requires a higher experimental accuracy.

The evolution with temperature of the shape and the intensity of the enlarged sextuplet shows the existence of clusters with a distribution of relaxation times, evolving with decreasing temperature.

An exact value of the freezing temperature corresponding to the time constant of the Mössbauer experiment ($\tau = 2 \times 10^{-8}$ s) cannot be deduced. However, the blocking temperatures of the different clusters should be distributed around T_f , which can be roughly estimated from the temperature corresponding to the inflection point ($T \approx 3.3$ K) in the curve shown in Fig. 17. This temperature is higher than the temperature of the susceptibility maximum (i.e., $T_f = 2.50$ K for $\nu = 17$ Hz), reflecting the existence of a dynamical effect. On the other hand, the observed H_{hyp} distribution at low temperature is coherent

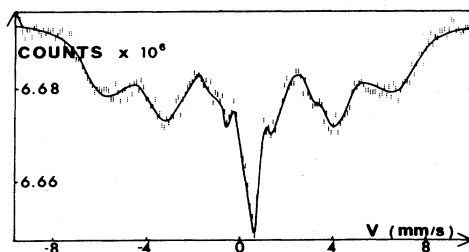


FIG. 16. Mössbauer spectrum at $T=2.27$ K.

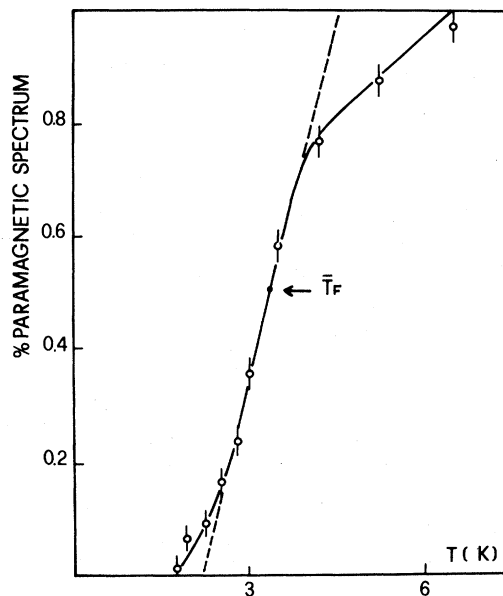


FIG. 17. Temperature variation of the percentage of paramagnetic Mössbauer spectrum.

with spin-glass-type order.

The appearance of the hyperfine pattern at $T=6.5$ K should be due to the persistence, at this chromium concentration, of a small residual antiferromagnetic framework (involving a fraction of spins too low to give detectable magnetic reflections in neutron-diffraction spectra). Indeed, this temperature is coherent with the ordering temperatures measured for $x \geq 0.85$ (Ref. 28), and the H_{hyp} distribution, at 4.2 and 5.0 K, shows a maximum at about 440 kOe, a value close to that found for $x \geq 0.85$ (Ref. 28). The order is probably very disturbed (see below) and the population of these antiferromagnetically ordered spins is about 10%. At lower temperature this order should be destroyed because no asymmetry is detected at $T=1.8$ K in the H_{hyp} distribution.

A preliminary spectrum performed at $T=4.2$ K with an applied field of 60 kOe shows that the intensity of the paramagnetic doublet is strongly reduced, replaced by a relaxing hyperfine spectrum (with relaxation times distributed around 10^{-8} s). No important modification in the shape of the enlarged sextuplet is observed. Therefore the spin direction is not defined, indicating that antiferromagnetic order is very perturbed; we are probably in the presence of a random, canted structure. On the other hand, the magnetic field produces an energy barrier determining an increase of the relaxation time of the different clusters and, therefore, the intensity of the enlarged sextuplet increases. The shape of the sextuplet, however, does not change with the applied field, but it is different from that observed at $T=1.8$ K. The resulting order is therefore different. Additional experiments are in progress in an attempt to elucidate this point.

Our results are not inconsistent with the presence of entropic clusters, whose relaxation time is temperature independent, if their number is less than 2%, in agreement with the estimation from susceptibility measurements.

H. EPR spectra

The room-temperature signal consists of a strong symmetrical absorption with $g=1.99$. The line shape is Lorentzian and the spectrum is attributed to large clusters of chromium ions coupled by exchange.²⁵ The temperature dependence of the peak-to-peak linewidth ΔH_{pp} is reported in Fig. 18 down to $T=60$ K. Below this temperature the signal is almost lost because of strong antiferromagnetic interactions present in the system. The line broadens continuously from $T=300$ to 60 K, as observed in other spin-glasses approaching T_f .^{55,56}

In the temperature range $120 \leq T \leq 300$ K an analysis of the line shape has been performed assuming the analytical expressions of the first derivative for a Gaussian and a Lorentzian absorption line.¹³ The signal remains Lorentzian down to $T=120$ K, and the relaxation rate τ^{-1} can be calculated⁵⁷ from the equation $\gamma\Delta H = \chi_T^{-1}\omega_a^2\tau$. The results indicate that the criterion $\omega_0\tau \ll 1$ is valid in this temperature range and, therefore, we ascribe the increase in ΔH_{pp} to a slowing down of the spin fluctuations.

Below $T=120$ K the linewidth increases more rapidly as the temperature decreases, but, unfortunately, the very low intensity of the signal prevents an accurate analysis of the line shape. Therefore we cannot correlate the phenomenon to a failure of the exchange-narrowing model as observed in $\text{CdIn}_{2-2x}\text{Cr}_{2x}\text{S}_4$.¹³ The lack of shift of the resonant field down to $T=60$ K may be related to the very high ratio $T/T_f \approx 25$.

A study of the temperature dependence of the relative number of the spins IT (area resonance multiplied by the temperature) clearly indicates the antiferromagnetic character of the magnetic correlations and their progressive evolution with decreasing temperature (Fig. 19). These magnetic correlations seem to play a role even at room temperature; the product IT does not reach a constant

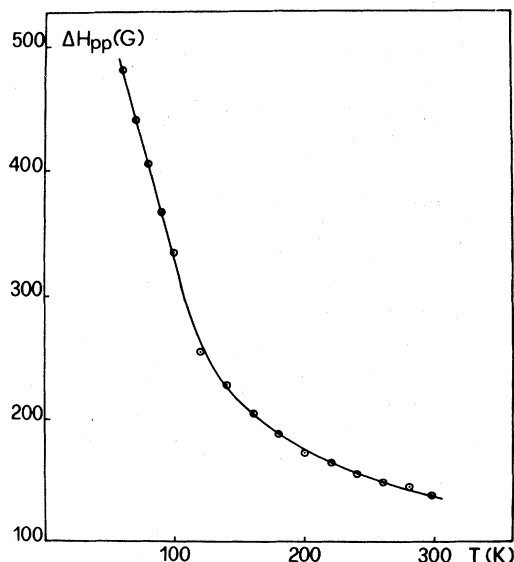


FIG. 18. Temperature dependence of the ΔH_{pp} linewidth of the EPR signal.

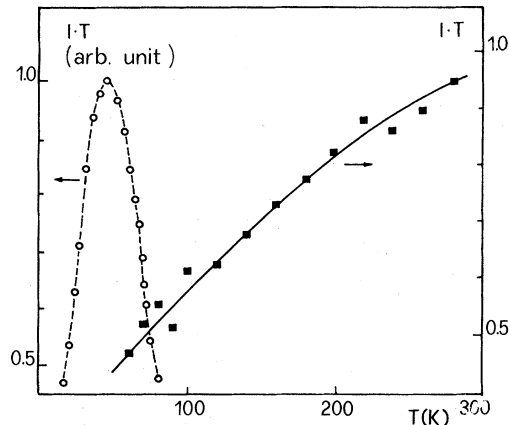


FIG. 19. Temperature dependence of IT (area of resonance multiplied by temperature) for $\text{ZnCr}_{1.6}\text{Ga}_{0.4}\text{O}_4$ (■) and for $\text{CdCr}_{1.6}\text{In}_{0.4}\text{S}_4$ (○) reported for comparison (from Ref. 12) in the EPR spectra.

value as expected for a well-behaved paramagnet without low-energy excited states and if $h\nu \ll KT$. This hypothesis is in agreement with the neutron-diffraction data.

Figure 19 reports, for comparison, the IT -versus- T behavior for the thiospinel spin-glass with the same chromium concentration $\text{CdCr}_{1.6}\text{In}_{0.4}\text{S}_4$, where the NN ferromagnetic interactions predominate over the NNN antiferromagnetic interactions.¹²

IV. CONCLUSIONS

We have reported experimental evidence of spin-glass behavior in the antiferromagnetic frustrated spinel $\text{ZnCr}_{1.6}\text{Ga}_{0.4}\text{O}_4$ using low-field dc- and ac-susceptibility measurements, neutron-diffraction experiments, Mössbauer and EPR spectra.

The antiferromagnetic order observed in the pure compound ($x=1$) persists down to $x=0.85$. Then it stabilizes into a spin-glass phase which we have characterized in this paper. This kind of behavior corresponds to the general phase diagram proposed by Poole and Farach.²²

The system is highly concentrated in magnetic ions (80% of octahedral sites occupied by chromium ions). It is characterized by strong short-range antiferromagnetic interactions, with short-range magnetic order present up to temperatures much higher than the freezing temperature, as evidenced by neutron-diffraction spectra. This is confirmed by susceptibility measurements, where a deviation from the Curie-Weiss law is observed at high temperatures, and EPR spectra, where there is a continuous increase of the linewidth with decreasing temperature.

As the temperature decreases, the antiferromagnetic short-range order evolves towards a collective freezing at T_f ($=2.50$ K at $\nu=17$ Hz).

The presence of irreversibility effects above the freezing temperature indicates the presence of uncompensated clusters, some of them frozen above T_f . This is coherent with the existence of clusters with a distribution of relaxation times, suggested by Mössbauer spectra, which show a large hyperfine pattern appearing at $T=6.5$ K and in-

creasing continuously in intensity down to $T=1.8$ K.

Below $T=1$ K a paramagnetic behavior of the susceptibility has been found, revealing the existence of unfrozen clusters of different dimension, including single ions. These clusters have been suggested to be entropic-type clusters resulting from the frustration. They experience a zero effective field, due to interactions with their neighbors, and therefore give a Curie-type contribution to the observed susceptibility. The proportion of such clusters should increase with the number of frustrated bonds and therefore would be strongly concentration dependent. The study of the evolution of the very-low-temperature magnetic properties, as a function of the composition, of the complete system $\text{ZnCr}_{2x}\text{Ga}_{2-2x}\text{O}_4$, is actually in progress and should permit us to develop the above-reported concepts.

ACKNOWLEDGMENTS

One of us (D.F.) is indebted to the Centre de Recherches sur les très basses Températures (Centre National de la Recherche Scientifique), Grenoble, where the low-field susceptibility measurements were performed during a stay [supported by North Atlantic Treaty Organization (NATO)]. We thank Dr. J. L. Soubeyroux for his valuable assistance in the analysis of the neutron-scattering data. Helpful discussions with Dr. K. Matho and Dr. R. Rammal are gratefully acknowledged. Thanks are due to Mr. P. Filaci for assistance with high-field susceptibility measurements and to Mr. P. Renaudin for his assistance in Mössbauer experiments. Finally we thank the Consiglio Nazionale delle Ricerche (Italy) for financial assistance (Grant No. 10434/03/8102536).

- ¹G. Toulouse, *Comments Phys.* **2**, 115 (1977).
- ²H. Maletta and W. Felsch, *Phys. Rev. B* **20**, 1245 (1979).
- ³R. R. Galazka, Schichi Nagata, and P. H. Keesom, *Phys. Rev. B* **22**, 3344 (1980).
- ⁴M. Escorne, A. Mauger, R. Triboulet, and J. L. Tholence, *Physica (Utrecht)* **107B**, 309 (1981).
- ⁵M. Escorne and A. Mauger, *Phys. Rev. B* **25**, 4674 (1982).
- ⁶Shoichi Nagata, R. R. Galazka, D. P. Mullin, H. Akbarzadeh, G. D. Khattk, J. K. Furdyna, and P. H. Keesom, *Phys. Rev. B* **22**, 3331 (1980).
- ⁷L. De Seze, *J. Phys. C* **10**, 2353 (1977).
- ⁸J. Villain, *Z. Phys. B* **33**, 31 (1979).
- ⁹M. Alba, J. Hammann, and M. Nogues, *Physica (Utrecht)* **107B**, 627 (1981).
- ¹⁰M. Alba, J. Hammann, and M. Nogues, *J. Phys. C* **15**, 5441 (1982).
- ¹¹M. Nogues, A. Saifi, M. Hamedoun, J. L. Dormann, A. Malmanche, D. Fiorani, and S. Viticoli, *J. Appl. Phys.* **53**, 7699 (1982).
- ¹²D. Fiorani, M. Nogues, and S. Viticoli, *Solid State Commun.* **41**, 537 (1982).
- ¹³S. Viticoli, D. Fiorani, M. Nogues, and J. L. Dormann, *Phys. Rev. B* **26**, 11 (1982).
- ¹⁴D. Fiorani, S. Viticoli, J. L. Dormann, M. Nogues, J. L. Tholence, J. Hammann, and A. P. Murani, *J. Magn. Magn. Mater.* **31-34**, 947 (1983).
- ¹⁵P. W. Anderson, *Phys. Rev.* **102**, 1008 (1956).
- ¹⁶R. Plumier, M. Lacomte, and M. Sougi, *J. Phys. (Paris) Lett.* **38**, L149 (1977).
- ¹⁷F. Hartmann-Boutron, A. Gerard, P. Imbert, R. Kleinberger, and F. Varret, *C. R. Acad. Sci. Ser. B* **268**, 906 (1969).
- ¹⁸R. Plumier, thèse d'état, University of Paris, 1968.
- ¹⁹A. Olés, *Phys. Status Solidi A* **3**, 569 (1970).
- ²⁰R. Plumier, *C. R. Acad. Sci. Ser. B* **267**, 98 (1968).
- ²¹F. K. Lotgering, *J. Phys. (Paris) Colloq.* **32**, C1-34 (1971).
- ²²C. P. Poole, Jr. and H. A. Farach, *Z. Phys. B* **47**, 55 (1982).
- ²³P. K. Baltzer, P. J. Woytowicz, M. Robbins, and E. Lopatin, *Phys. Rev.* **151**, 367 (1966).
- ²⁴D. Fiorani, L. Gastaldi, A. Lapicciarella, S. Viticoli, and N. Tomassini, *Solid State Commun.* **32**, 831 (1979).
- ²⁵F. Scholl and K. Binder, *Z. Phys. B* **39**, 239 (1980).
- ²⁶F. Gesmundo, *Nuovo Cimento* **25**, 795 (1975).
- ²⁷C. Battistoni, J. L. Dormann, D. Fiorani, E. Paparazzo, and S. Viticoli, *Solid State Commun.* **39**, 581 (1981).
- ²⁸D. Fiorani, S. Viticoli, J. L. Dormann, J. L. Tholence, J. Hammann, A. P. Murani, and J. L. Soubeyroux, *J. Phys. C* **16**, 3175 (1983).
- ²⁹J. L. Tholence, thèse d'état, University of Grenoble, 1973.
- ³⁰D. Fiorani and S. Viticoli, *J. Solid State Chem.* **26**, 101 (1979).
- ³¹J. L. Tholence, *J. Appl. Phys.* **50**, 7308 (1979).
- ³²F. Holtzberg, J. L. Tholence, H. Godfrin, and R. Tournier, *J. Appl. Phys.* **50**, 1717 (1979).
- ³³G. Eiselt, J. Kötzer, H. Maletta, K. Binder, and D. Stauffer, *J. Magn. Magn. Mater.* **13**, 146 (1979).
- ³⁴G. Eiselt and J. Kötzer, *J. Magn. Magn. Mater.* **15-18**, 191 (1980).
- ³⁵A. J. Bray, M. A. Moore, and P. J. Reed, *J. Phys. C* **11**, 1187 (1978).
- ³⁶R. Rammal, R. Suchail, and R. Maynard, *Solid State Commun.* **32**, 487 (1979).
- ³⁷S. Nagata, P. H. Keesom, and H. R. Harrison, *Phys. Rev. B* **19**, 1633 (1979).
- ³⁸H. von Löhneysen, J. L. Tholence, and F. Steglich, *Z. Phys. B* **29**, 319 (1978).
- ³⁹E. C. Hirshkoff, O. G. Symko, and J. C. Wheatly, *J. Low Temp. Phys.* **5**, 155 (1971); J. O. Thomson and J. R. Thompson, *Physica (Utrecht)* **107B**, 637 (1981), and references therein.
- ⁴⁰J. L. Tholence, *Solid State Commun.* **35**, 113 (1980).
- ⁴¹J. L. Tholence, *Physica (Utrecht)* **108B**, 1287 (1981).
- ⁴²C. A. M. Mulder, A. J. van Duyneveldt, and J. A. Mydosh, *Phys. Rev. B* **23**, 1384 (1981).
- ⁴³C. A. M. Mulder and A. J. van Duyneveldt, *Physica (Utrecht)* **113B**, 123 (1982).
- ⁴⁴D. Fiorani, J. L. Tholence, and J. L. Dormann, *Physica (Utrecht)* **107B&C**, 643 (1981).
- ⁴⁵D. Fiorani, J. L. Tholence, and J. L. Dormann, *J. Magn. Magn. Mater.* **31-34**, 947 (1983).
- ⁴⁶J. L. Dormann, D. Fiorani, J. L. Tholence, C. Sella, *J. Magn. Magn. Mater.* **35**, 117 (1983).
- ⁴⁷K. Binder, *J. Phys. (Paris)* **39**, 2 (1978).
- ⁴⁸J. Ferré, J. Rajchenbach, and H. Maletta, *J. Appl. Phys.* **52**, 1697 (1981).
- ⁴⁹J. Rajchenbach, thèse de Troisième cycle, University of Paris, 1980.
- ⁵⁰J. L. Tholence and R. Tournier, *Physica* **86-88B**, 837 (1977).
- ⁵¹J. J. Prejan and J. Souletie, *J. Phys. (Paris)* **41**, 1335 (1980).
- ⁵²C. Chappert, thèse de Troisième cycle, University of Paris,

- 1980.
- ⁵³H. von Löhneysen and J. L. Tholence, *Phys. Rev. B* **19**, 5858 (1979).
- ⁵⁴K. R. A. Ziebeck, P. J. Brown, and J. Phys. F **10**, 2015 (1980);
K. R. A. Ziebeck, P. J. Brown, J. H. Booth, and J. A. C. Bland, *ibid.* **11**, 2127 (1981).
- ⁵⁵J. P. Jamet and A. P. Malozemoff, *Phys. Rev. B* **18**, 75 (1978).
- ⁵⁶J. P. Jamet, J. V. Dumais, J. Seiden, and K. Knorr, *J. Magn. Mater.* **15-18**, 197 (1980).
- ⁵⁷M. B. Salamon, *Solid State Commun.* **31**, 781 (1979).